Pergamon

Cement and Concrete Research 32 (2002) 1705–1716

CEMENT AND CONCRETE RESEARCH

Microstructural characterisation of geopolymers synthesised from kaolinite/stilbite mixtures using XRD, MAS-NMR, SEM/EDX, TEM/EDX, and HREM

Hua Xu, Jannie S.J. Van Deventer*

Department of Chemical Engineering, University of Melbourne, Melbourne, Victoria 3010, Australia

Received 6 February 2001; accepted 3 May 2002

Abstract

When crystalline aluminosilicates partially dissolve in a concentrated alkaline medium, an amorphous geopolymeric gel is formed interspersed with undissolved crystalline particles. Some aluminosilicates dissolve more readily than others to give an equilibrium ratio of aluminium to silicon in the gel. In this case study, kaolinite and stilbite mixtures were used to investigate the relative reactivity of different minerals when present in different ratios. XRD and ^{29}Si and ^{27}Al MAS-NMR were used to determine when a specific mineral was completely transferred into the gel phase. Electron diffraction using transmission electron microscopy (TEM) and high-resolution transmission electron microscopy (HREM) were employed to establish the amorphous nature of the gel phase. Scanning electron microscopy (SEM)/energy dispersive X-ray (EDX) and TEM/EDX were then used to determine the composition of the gel. By using simple mass balance assumptions, the quantity of gel and the extent of partial dissolution of an aluminosilicate could then be calculated. It was found that a geopolymer containing a higher weight percentage of CaO in its gel, a lower ratio of (average surface area)/gel, and where the undissolved crystalline particles have a higher hardness had higher mechanical strength. The method developed in this paper is also applicable to other cementitious materials.

Keywords: Geopolymer; Amorphous material; Characterisation; SEM; TEM

1. Introduction

Invented by Davidovits in the late 1970s [1,2], geopolymers are amorphous to semicrystalline three-dimensional aluminosilicate polymers. Geopolymerisation occurs in highly alkaline solution with aluminosilicate oxides and silicates (either solid or liquid) as the reactants. As a result of their excellent mechanical properties and fire and acid resistance, geopolymeric products have been investigated for their potential application in industry for more than 20 years [1–10]. Geopolymeric reactants could range from kaolinite or metakaolinite [1–4] to a group of materials containing rich SiO_2 and/or Al_2O_3 oxides, e.g., fly ash, slag, construction waste, and natural minerals [5–10].

Davidovits [2] reported the structural characterisation of geopolymeric binders by XRD and MAS-NMR in 1994. It should be noted that the geopolymeric binders (polysialate, polysialate-siloxo, and polysialate-disoloxo) characterised by Davidovits [2] were evenly dispersed amorphous to semicrystalline products synthesised at a temperature higher than 100 °C and pressure higher than atmosphere using kaolinite or calcined kaolinite as the sole aluminosilicate source. In contrast, most geopolymers synthesised from different starting materials are mixtures of crystalline aluminosilicate particles and semicrystalline and amorphous aluminosilicate gel. Due to the complex composition of such geopolymers and the difficulties of separating the crystalline aluminosilicates particles from the semicrystalline and amorphous gel phases, characterisation of the structural composition of geopolymers has not been conducted as yet.

As a mixture of amorphous to semicrystalline and crystalline phases, the mechanical strength of a geopolymer should be the result of both the amorphous gel phase as binder and the crystalline aluminosilicate particles as filler. Hence, an understanding of the structural composition as well as the gel phase of a geopolymer will aid the development of improved geopolymers.

* Corresponding author. Tel.: +61-3-8344-6620; fax: +61-3-8344-4153.
E-mail address: jannie@unimelb.edu.au (J.S.J. Van Deventer).

0008-8846/02/$ – see front matter © 2002 Elsevier Science Ltd. All rights reserved.
PII: S0008-8846(02)00859-1

XRD, MAS-NMR, scanning electron microscopy (SEM)/energy dispersive X-ray (EDX), and transmission electron microscopy (TEM)/EDX techniques have been used previously to characterise cement, concrete, fly ash, zeolites, and clay [11–19]. However, most of this work has involved qualitative or semiquantitative analysis of crystalline materials [11,13,15,17,18]. By using SEM/EDX, Davies and Oberholster [12] carried out a semiquantitative analysis of both the crystalline and amorphous phases for the surfaces of concrete and mortar specimens. Also, Enders [16] characterised separate glassy and anhydrate fly ash particles by combining AEM and EDX techniques. Nevertheless, it has been noted that neither Davies and Oberholster's nor Ender's work was aimed at characterising the bulk structural composition with respect to the crystalline and amorphous phases.

The objective of this paper is to develop an approach for semiquantitative characterisation of the geopolymeric materials possessing both crystalline and amorphous phases. XRD, MAS-NMR, SEM/EDX, TEM/EDX, and high-resolution transmission electron microscopy (HREM) techniques have been applied to analyse the structure of the geopolymers synthesised from stilbite/kaolinite mixtures. Stilbite ($NaCa_4(Si_{27}Al_9)O_{72}\cdot 30H_2O$) is a natural zeolite having high reactivity in geopolymerisation, while kaolinite has been shown to contribute relatively high concentration of aluminium to the gel phase. It will be shown that mixtures of minerals present new insight into the effect of mineral reactivity on geopolymer microstructure that which is not possible using single minerals. The effect of structural composition on mechanical strength of the geopolymer has also been considered.

2. Experimental procedure

2.1. Geopolymers synthesised from kaolinite/stilbite mixture

Stilbite obtained from Geological Specimen Supplies, New South Wales, Australia, was ground to -80 μm. The mean density and hardness of the stilbite are 2.21 g/cm^3 and 4.0 Mohs, respectively [20]. Kaolinite, grade HR1/F, was purchased from Commercial Minerals, Sydney, Australia with a particle size of 1% >38 μm. The mean particle sizes for stilbite and kaolinite detected by a COULTER LS particle size analyser are 23.05 and 5.8 μm, respectively. The mean density and hardness of kaolinite are 2.62 g/cm^3 and 2.5 Mhos, respectively [20]. The compositions of stilbite and kaolinite were determined by X-ray fluorescence (XRF) analysis with results listed in Table 1. Clay (CMS KGa-1) is a well-crystallised kaolinite from Georgia, USA and obtained from the Source Clay Repository, Department of Geology, University of Missouri, Columbia, MO, USA. Sodium silicate solution (Vitrosol N40) with density of 1.385 g/ml was supplied by PQ Australia, and contained 28.65 wt.% of SiO_2. Distilled water and analytical grade NaOH were used throughout all experiments.

Table 1
Composition of kaolinite and stilbite as determined by XRF analysis (mass%)

Element as oxide	Kaolinite HR1/F	Stilbite
SiO_2	54.5	59.2
Al_2O_3	29.4	14.8
MgO	0.2	0.07
Fe_2O_3	1.4	0.23
CaO	0.2	7.65
K_2O	0.2	0.03
Na_2O	0.2	0.18
TiO_2	2.8	0.03
Loss on ignition	11	15.87

Table 2
Compressive strength of geopolymers synthesised by kaolinite/stilbite matrix

Geopolymer	Kaolinite/stilbite (mass ratio)	MPa
G1	6.5	2.3
G2	0.5	7.8
G3	0.1	9.5

A total of 21 g of kaolinite and stilbite powder were dry mixed at a kaolinite/stilbite mass ratio of 6.5 (G1), 0.5 (G2), and 0.1 (G3) for 10 min before the addition of 1.3 ml of sodium silicate and 6 ml of 5 M NaOH solutions. Each of the subsequent mixtures was mixed by hand for a further 5 min and then transferred to a steel mould measuring $20 \times 20 \times 20$ mm. After being left in an oven for 3 days at 35 °C, the compressive strengths for these three samples were tested using a Tinus Tolsen compressive strength testing machine.

Geopolymers synthesised from kaolinite/stilbite mixtures show differences in mechanical strength when different kaolinite/stilbite mass ratios are applied. It is assumed that a higher strength geopolymer is associated with a more desirable internal microstructure. A series of samples with kaolinite/stilbite mass ratios changing from 9.0 to 0.1 were investigated. An incremental increase in mechanical strength was observed as the kaolinite/stilbite mass ratio decreased. However, the geopolymer obtained at a kaolinite/stilbite mass ratio of "0" shows a lower compressive strength than that synthesised at a kaolinite/stilbite mass ratio of 0.1 (G3). Therefore, three geopolymers synthesised at kaolinite/stilbite mass ratios of 6.5 (G1), 0.5 (G2), and 0.1 (G3) were selected for investigation in the present work, with compressive strength given in Table 2. These compositions and matrices have not been selected to give optimal strengths, but rather to demonstrate the process principles involved.

2.2. XRD and MAS-NMR analyses

X-ray powder diffraction work was recorded on a Philips PW 1800 spectrometer using Cu K_α Radiation (40 kV, 30 mA) with a scanning rate of 2°/min from 5°

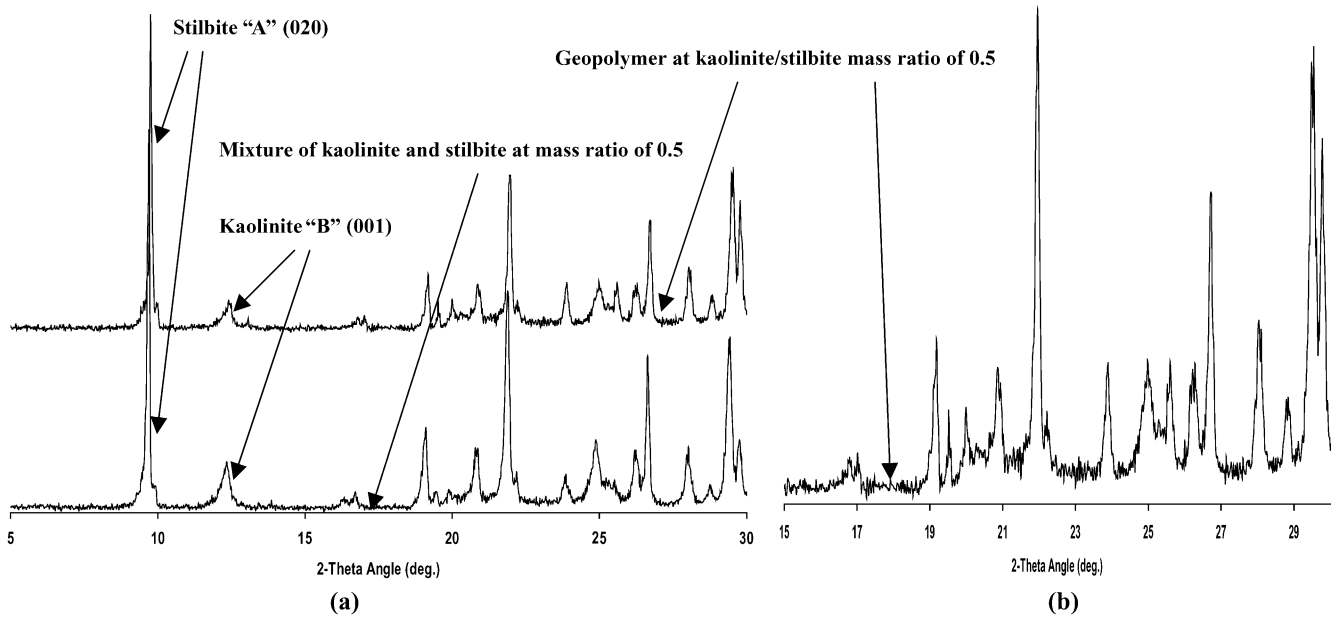

Fig. 1. XRD patterns: (a) geopolymer and powder mixture of kaolinite and stilbite at the mass ratio of 0.5 (2θ = 5–30) and (b) geopolymer of kaolinite and stilbite at the mass ratio of 0.5 (2θ = 15–30).

to 70° (2θ). As the kaolinite characteristic and stilbite characteristic peaks are located at less than 30° (2θ), the XRD patterns (Figs. 1–3) recorded for kaolinite, stilbite, and the geopolymers synthesised from kaolinite/stilbite mixtures are shown from 5° to 30° (2θ).

The ^{29}Si and ^{27}Al MAS-NMR spectra were obtained at 59.61 and 78.18 MHz on a Varian 300/solid-state spectrometer employing magic angle spinning at 6.9 kHz. The NMR peaks are fitted by Gaussian lines.

2.3. SEM, TEM, and HREM analyses

A JEOL JSM-840 microscope with Tracor Northern EDAX system was used for SEM/EDX analysis at the accelerating voltage of 20 kV. A JEOL JSM-6300F field emission gun SEM (FEG SEM) was also used for image observation of the samples at the accelerating voltage of 5 kV. Samples for both JSM-840 and JSM-6300F analyses were placed on the sample holders supported by carbon paint followed by 1-min sputter coating of gold.

TEM/EDX analyses were conducted on a Philips EM 420 TEM at the accelerating voltage of 100 kV. The X-ray counts were obtained by integrating K_α X-ray peaks using an EDAX PV 9900 EDX microanalyser. The accuracy of the system was tested with kaolinite (CMS KGa-1) and the systematic error was found to be less than 5% compared to the ideal composition of the kaolinite (CMS KGa-1).

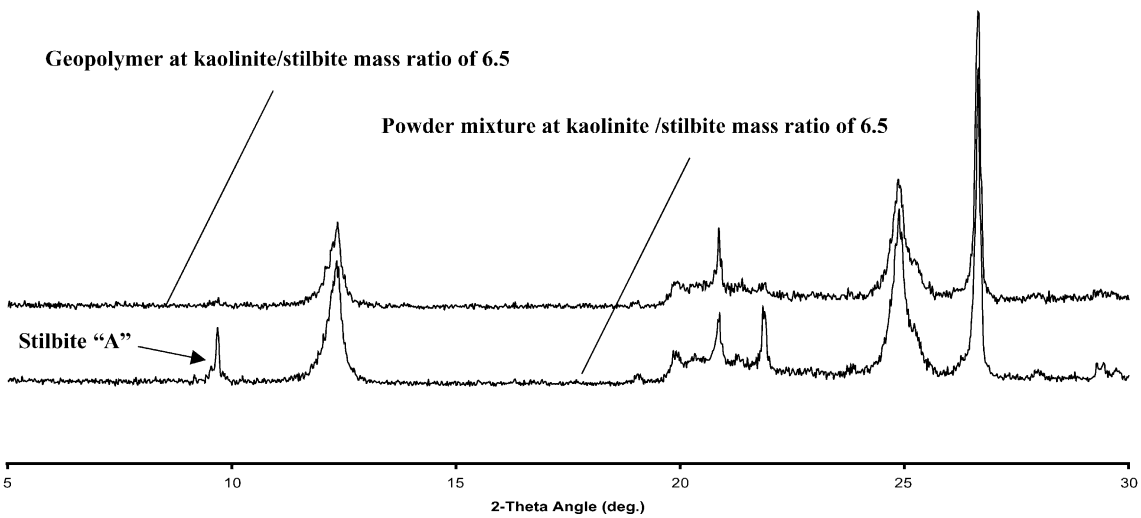

Fig. 2. XRD patterns of geopolymer with kaolinite/stilbite mass ratio of 6.5 and the powder mixture of kaolinite and stilbite with the same mass ratio.

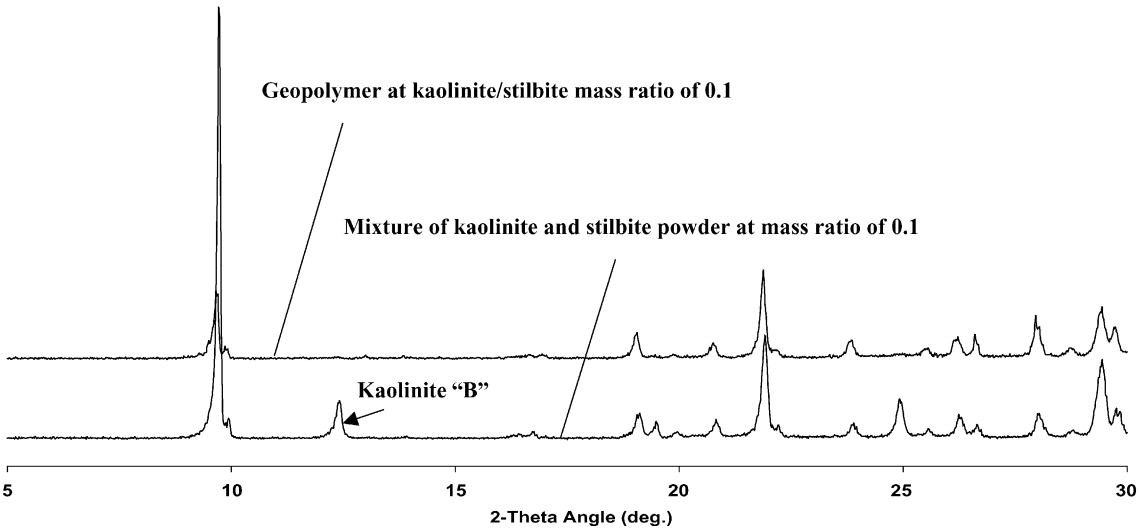

Fig. 3. XRD patterns of geopolymer with kaolinite/stilbite mass ratio of 0.1 and the powder mixture of kaolinite and stilbite with the same mass ratio.

A JEOL JEM-400EX HREM was used to observe the microstructure of geopolymers G1 and G3. Samples investigated by both TEM and HREM were prepared by grinding bulk specimens and depositing particles from an alcohol suspension on carbon-covered copper grids. The size range of particles analysed is 500–1000 nm so that the absorption of fluorescence and X-ray from the specimen can be neglected.

3. Results and discussion

3.1. XRD analysis

Figs. 1–3 show the powder X-ray diffraction patterns of mixtures and geopolymers at the kaolinite/stilbite mass ratio of 0.5, 6.5, and 0.1, respectively. It is found from Fig. 1 that for the geopolymer synthesised at a kaolinite/stilbite mass ratio of 0.5 (G2), both the stilbite (020) peak "A" and the kaolinite (001) peak "B" are detectable, despite these two peaks being significantly lower in intensity after the geopolymerisation. This observation means that G2 contains both crystalline kaolinite and stilbite particles. It is also worthy to note that no new crystalline peak can be detected in any XRD patterns recorded for geopolymers G1, G2, and G3. Consequently, the gel phases formed during the geopolymerisation of the kaolinite and stilbite are probably amorphous to semicrystalline in structure. The reason that the typical amorphous halo shape has not been observed in Figs. 1(a), 2, and 3 could be attributed to the extraordinarily high intensity of the stilbite peak (thousands higher in intensity), which depresses the relative value of the amorphous signals. Moreover, a comparatively small amount of the gel phase embodied in the bulk geopolymers (G1, G2, and G3) could be another reason for the gel phase to be observed as the increased background, rather than an obvious halo shape. Nevertheless, when the most intensive peak (020) of the stilbite is removed from the XRD pattern (Fig. 1(b)), an obviously increased background in Fig. 1(b) indicates that G2 comprises crystalline kaolinite and stilbite particles and amorphous to semicrystalline gel phase.

Fig. 2 shows the XRD pattern of the geopolymer synthesised at a kaolinite/stilbite mass ratio of 6.5 (G1). An XRD pattern for the powder mixture of kaolinite and stilbite before geopolymerisation at the same mass ratio of 6.5 is also given in Fig. 2. It is noted that no stilbite characteristic peak "A" is observed for the geopolymer so that a complete transfer of stilbite particles from the crystalline phase to the amorphous gel phase is assumed to occur in the geopolymerisation of G1. For the geopolymer synthesised at a kaolinite/stilbite mass ratio of 0.1 (G3), the corresponding XRD pattern (Fig. 3) contains only stilbite characteristic peaks. The disappearance of the kaolinite characteristic peak "B" in Fig. 3 implies a complete dissolution of crystalline kaolinite particles during the geopolymerisation of G3.

Consequently, different structural compositions were observed for G1, G2, and G3, of which G1 consisted of crystalline kaolinite particles and amorphous gel, G2 possessed both crystalline kaolinite and stilbite particles as well as gel phase, and G3 was composed of crystalline stilbite particles and gel phase. It is also noteworthy that there is no new peak found in the XRD patterns recorded for G1, G2, and G3, which demonstrates that there is no new crystalline phase formed during the geopolymerisation of G1, G2, and G3.

3.2. MAS-NMR analysis

Table 3 and Fig. 4 describe the chemical shifts of ^{27}Al and ^{29}Si MAS-NMR for kaolinite, stilbite, G1, G2, and G3. It is observed that the ^{27}Al and ^{29}Si MAS-NMR signals for

Table 3
^{27}Al and ^{29}Si MAS-NMR chemical shifts (ppm) of stilbite, kaolinite, and geopolymers synthesised from kaolinite/stilbite mixtures

Sample	Si(3Al)[a]	Si(2Al)[a]	Si(1Al)[a]	Si(0Al)[a]	Al(4Si)[a]	Al(3Si)[a]	Al[b]
Stilbite		− 98	− 101.5	− 111.3	59.1		
Kaolinite	− 91.6		− 100.3				2.3
G1	− 90		− 101.1	− 106.6		70.1	9.9
G2	− 92.4	− 98.8	− 102.3	− 114.9	58.7		1.8
G3		− 98.2	− 102.1	− 110.7	57.9		

G1: Geopolymer synthesised at the kaolinite/stilbite mass ratio of 6.5. G2: Geopolymer synthesised at the kaolinite/stilbite mass ratio of 0.5. G3: Geopolymer synthesised at the kaolinite/stilbite mass ratio of 0.1.

[a] Si(*n*Al) and Al(*n*Si) designate the SiO_4 and AlO_4 tetrahedrons connected to each other through shared oxygen atoms.

[b] Al associates with octahedral Al.

kaolinite and stilbite are different. In particular, kaolinite is structured by tetrahedral Si and octahedral Al atoms, while in stilbite both Si and Al atoms are tetrahedrally combined. The corresponding chemical shifts of ^{27}Al MAS-NMR for kaolinite and stilbite are therefore found at 2.3 and 59.1 ppm, respectively (Fig. 4). The substantial difference between the chemical shifts of ^{27}Al and ^{29}Si MAS-NMR for kaolinite and stilbite also suggests that the technique of ^{27}Al and ^{29}Si MAS-NMR can be used for interpreting the microstructure of the geopolymers synthesised from kaolinite/stilbite mixtures.

From Fig. 4, it is noted that the chemical shifts of ^{27}Al MAS-NMR obtained for G1 show both tetrahedral and octahedral Al atoms, of which the octahedral Al atom (9.9 ppm) can be interpreted as derived from kaolinite. The tetrahedral Al atom (70.1 ppm) observed in G1 is attributed to the Al atom structured in a three-dimensional Si–O–Al block of the gel phase. The chemical shift of ^{29}Si MAS-NMR found in G1 also represents the Si atom (− 90 ppm) present in kaolinite (Table 3).

In contrast with G1, G3 gives only tetrahedral ^{27}Al MAS-NMR signals at 57.9 ppm (Fig. 4) despite the background showing an increase compared with the unreacted kaolinite or stilbite. The ^{27}Al MAS-NMR signals at 57.9 ppm can be assigned to the undissolved stilbite particles. The ^{27}Al MAS-NMR signals of G3 (Fig. 4) show that no kaolinite particles can be detected in G3, because kaolinite will create characteristically an octahedral ^{27}Al MAS-NMR signal in the range of 0–10 ppm. The ^{27}Al MAS-NMR signals observed for G2 show both kaolinite and stilbite characteristic signals at 1.8 and 58.7 ppm, respectively, which indicates both kaolinite and stilbite remaining in G2.

However, it is worthy to indicate that the ^{27}Al and ^{29}Si MAS-NMR signals corresponding to the gel phase are not clearly detected in the geopolymers synthesised from kaolinite/stilbite matrices (Fig. 4). The possible reasons for this phenomenon could be as follows:

1. The formed gel phase is not abundant enough to show an identifiable peak as observed in G1 and G2 (Fig. 4); it appears as the background instead.

2. With the addition of Na_2SiO_3 and due to the higher SiO_2 than Al_2O_3 contained in both kaolinite and stilbite (Table 1), the Si/Al ratio in the formed gel phase is expected to be higher than 2. This higher Si/Al ratio in the gel phase means that the ^{29}Si MAS-NMR signals of the gel may appear only as a halo ranging from Si(2Al) to Si(Al), and to Si(0Al). Since both kaolinite and stilbite have comparatively stronger signals appearing in the same range (Table 3), the signals created by the gel phase cannot be detected clearly.

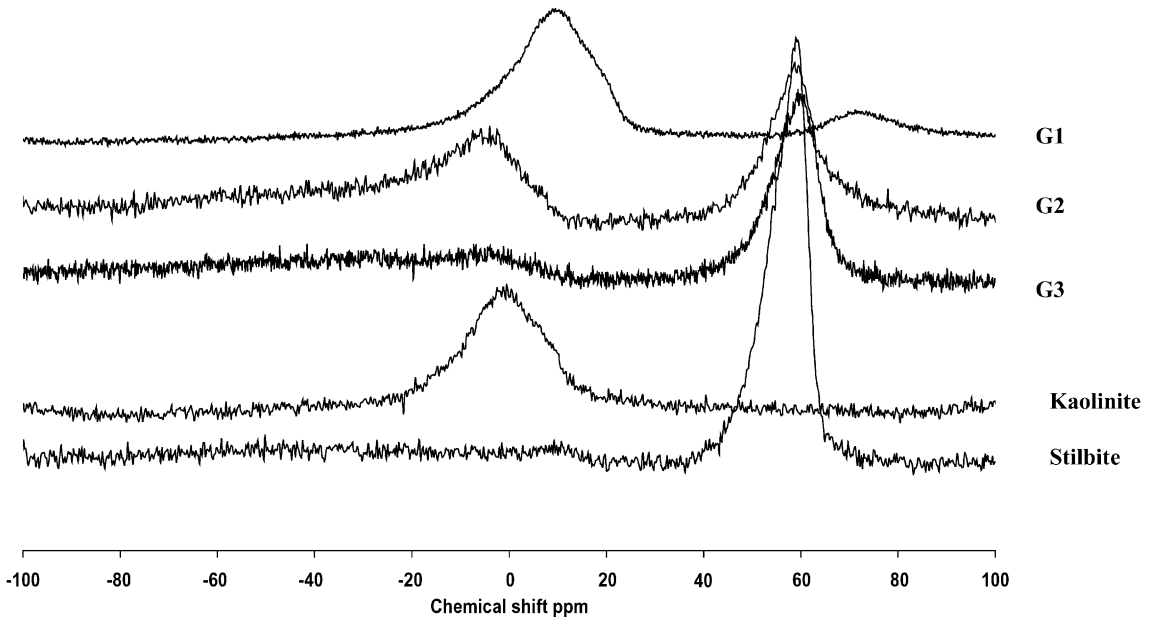

Fig. 4. The chemical shifts of ^{27}Al NMR recorded for stilbite, kaolinite, and geopolymers synthesised at the kaolinite/stilbite mass ratio of 6.5 (G1), 0.5(G2), and 0.1 (G3), respectively.

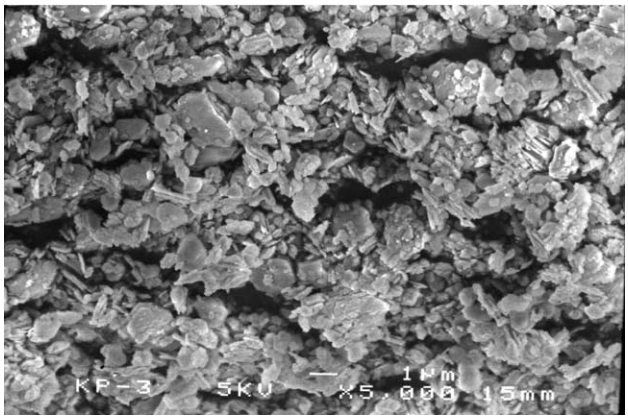

Fig. 5. SEM image of kaolinite powder.

In summary, the structural insight obtained from ^{27}Al and ^{29}Si MAS-NMR analyses for G1, G2, and G3 is in good agreement with the conclusions drawn from XRD analyses. G1 is a mixture of kaolinite particles and gel, G2 possesses both kaolinite and stilbite particles and gel, and G3 contains stilbite particles and gel. Such agreement demonstrates that both XRD and ^{27}Al and ^{29}Si MAS-NMR are reliable techniques for analysis of the structural composition in the present work.

3.3. SEM analysis

Figs. 5 and 6 are images of kaolinite and stilbite powder taken by a JSM-6300F FEG SEM. Kaolinite powder (Fig. 5) shows a layered hexagonal shape with particle size mostly smaller than 5 μm. Stilbite powder displays fourlings and triangle shapes with particle size mostly larger than 5 μm. The difference in appearance between crystalline kaolinite and stilbite particles could be used for distinguishing the kaolinite and stilbite particles during SEM and TEM investigations of G1, G2, and G3.

As mentioned earlier, geopolymers are often mixtures of aluminosilicate particles and gel phase. Such mixtures can also be observed from the SEM images of G1, G2, and G3. Figs. 7–9 are SEM images of the fractured surfaces of G1, G2 and G3 in which kaolinite particles (“A”) are detected under the gel layer on the broken surface of G1 (Fig. 7), while stilbite particles (“C”) as well as gel are found on the broken surface of G3 (Fig. 9). For G2 (Fig. 8), both kaolinite (“A”) and stilbite (“B”) particles are observed with the gel on the fractured surface. It is also noticed from Figs. 7–9 that G1 broke in the gel phase, while G2 and G3 fractured at the places where there was a deficiency of gel between particles. The observed difference between the broken surfaces of G1, G2, and G3 may suggest that G1 has a weaker gel than G2 and G3. The different amounts of the gel phase contained in G1, G2, and G3 may be another factor.

SEM/EDX analyses for the gel phases of G1, G2, and G3 were conducted at a magnification of 2000 at 15 different points in the gel phase. Table 4 lists the SEM/EDX results for the mean compositions of the gel phases of G1, G2, and G3. It is found from Table 4 that for G1 and G2, which started at the different kaolinite/stilbite mass ratios of 6.5 and 0.5,

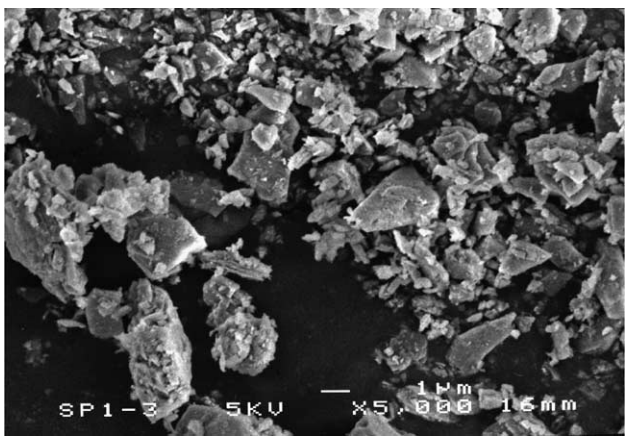

Fig. 6. SEM image of stilbite powder.

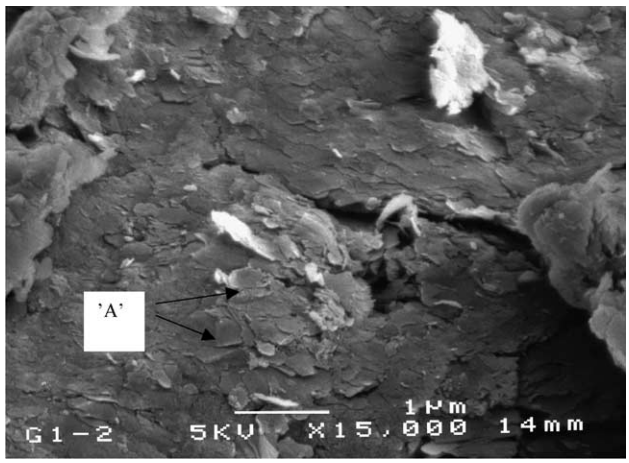

Fig. 7. SEM image of G1 with “A” showing kaolinite particles.

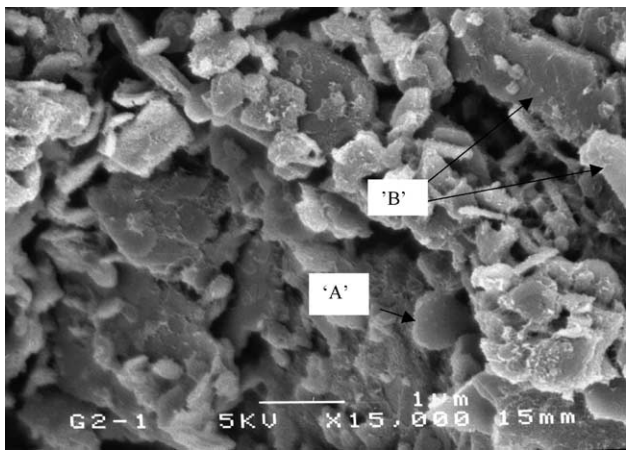

Fig. 8. SEM image of G2, with “A” showing kaolinite particle and “B” showing stilbite particle.

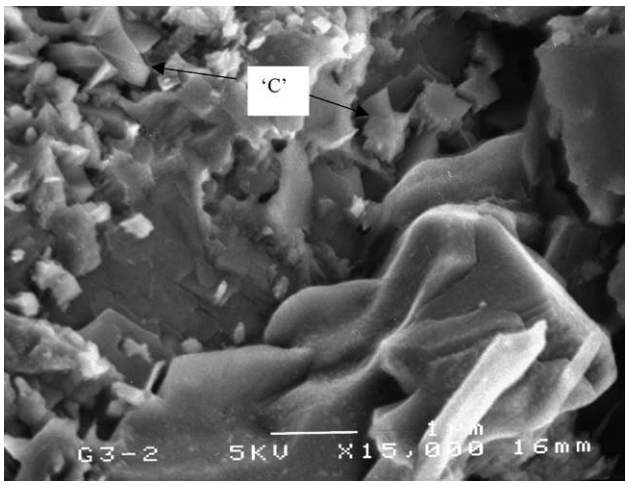

Fig. 9. SEM image of G3 with "C" showing stilbite particle.

respectively, the mean concentrations of Al_2O_3 weight percentage and SiO_2 weight percentage in the corresponding gels are very close to each other. This phenomenon suggests that an equilibrium of Al_2O_3 weight percentage and SiO_2 weight percentage may exist in the gel phases of G1 and G2. As the kaolinite and stilbite have different Al_2O_3 weight percentage and SiO_2 weight percentage contents, the different starting mass ratio (6.5 and 0.5) will, consequently, transfer different amounts of Al and Si species from kaolinite and stilbite into the gel phases to form gels with different Al_2O_3 weight percentage and SiO_2 weight percentage concentrations. Since similar Al_2O_3 weight percentage and SiO_2 weight percentage are observed in the gel phases of G1 and G2, it is assumed that a kind of equilibrium between Al_2O_3 weight percentage and SiO_2 weight percentage may affect the formation of the gel phases.

However, it is also noticed that the mean Al_2O_3 weight percentage detected from the gel phase of G3 (Table 4) is significantly lower than that contained in the gel phases of G1 and G2. As geopolymerisation of G3 is started at the kaolinite/stilbite mass ratio of 0.1, the lower mean Al_2O_3 weight percentage contained in the gel phase of G3 might be due to the lower content of Al_2O_3 weight percentage contained in stilbite (Table 1). The XRD and ^{27}Al MAS-NMR results showed that kaolinite was completely transferred into the gel phase of G3. Therefore, it can be deduced that an equilibrium is established between the Al_2O_3 weight percentage and SiO_2 weight percentage in the gel phase, but that such an equilibrium is based on certain conditions. In particular, one such condition may be that both Al_2O_3- and SiO_2-rich aluminosilicate sources should be available throughout the geopolymerisation. In the geopolymerisation of kaolinite and stilbite, kaolinite should be treated as an Al_2O_3-rich source and stilbite as a SiO_2-rich source. The complete dissolution of kaolinite particles during the geopolymerisation of G3 made the Al_2O_3-rich aluminosilicate source unavailable at some stage of the reaction, so that the Al_2O_3 weight percentage contained in the gel of G3 was

Table 4
Composition of gel phase in geopolymers (G1, G2, and G3) detected by SEM/EDX

Element as oxide (wt.%)	G1		G2		G3	
	Mean	S.D.	Mean	S.D.	Mean	S.D.
Al_2O_3	27.25	6.96	28.18	7.09	18.12	3.36
SiO_2	63.13	5.97	60.08	4.95	60.21	3.68
CaO	2.83	2.19	7.7	5.43	10.83	4.34
Na_2O	4.24	2.56	1.53	1.08	9.27	2.52
FeO	0.85	0.6	0.41	0.34	0.38	0.22
TiO_2	1.76	1.55	2.14	3.12	1.23	1.79

lower than the equilibrium Al_2O_3 weight percentage observed in G1 and G2.

Another observation from Table 4 is that the mean CaO weight percentage contained in the gel phase increased along with a decrease in the kaolinite/stilbite mass ratio in the geopolymerisation of G1, G2, and G3. From Table 1, kaolinite and stilbite are found to contain 0.2 and 7.65 wt.% of CaO, respectively, so that stilbite is the dominant mineral to dissolve CaO into the corresponding gel during geopolymerisation. In other words, the more stilbite involved in the geopolymerisation, the higher the CaO weight percentage observed in the corresponding gel. The CaO content of a source mineral was observed to enhance the mechanical strength of the resultant geopolymer [7], although the exact mechanism is not known. No cement related calcium silica hydrate phases were found in XRD analysis (Figs. 1–3), so that it can be assumed that the calcium forms part of the amorphous phase. G1 was observed to fracture in its gel phase at lower megapascal values, which may imply that the gel phase of G1 comprised of lower CaO weight percentage is weaker than the gel phases of G2 and G3. It is also noticed (Table 4) that the Na_2O weight percentage in the gel

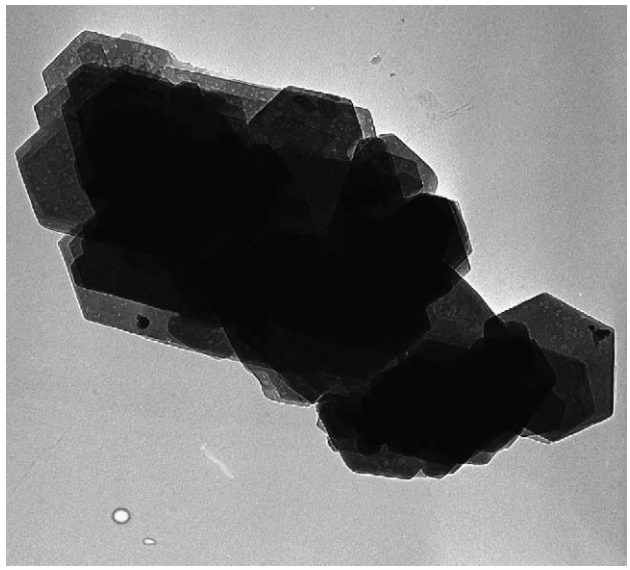

Fig. 10. TEM image of kaolinite at a magnification of $\times$ 36,300.

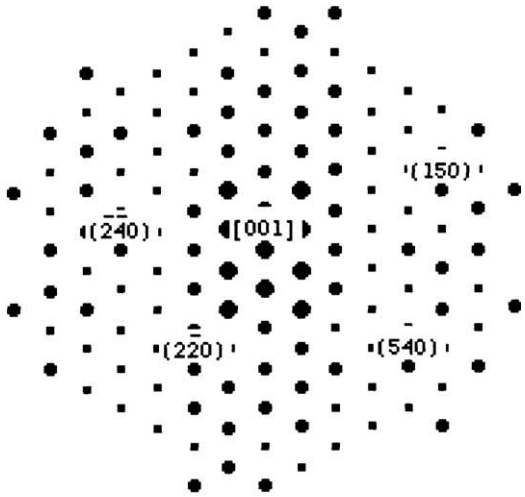

(a) Simulated DP of kaolinite

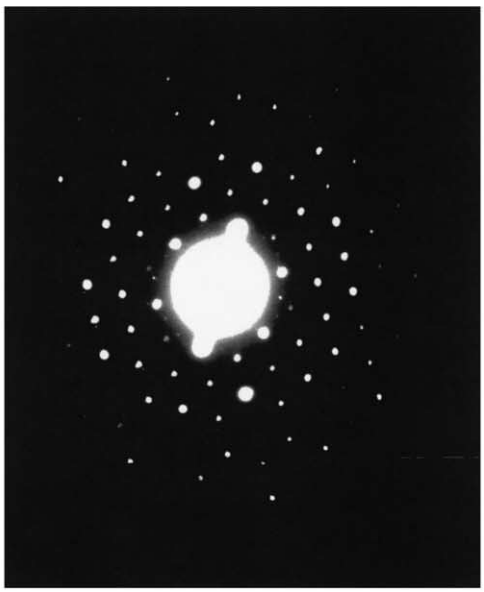

(b) DP of kaolinite

Fig. 11. Simulated and real DP of kaolinite particle.

phases of G1, G2, and G3 is 4.24, 1.53, and 9.27, respectively. The effect of Na_2O weight percentage contained in the gel phases on the compressive strength of the geopolymers or on the formation of the gel phases is not clear yet.

It should be noticed that the standard deviation (S.D.) of SEM/EDX analyses for G1, G2, and G3 shown in Table 4 is up to 7.09. The observation of these high S.D. values can be attributed to the rough fractured surfaces of the samples. Usually SEM/EDX analysis is conducted on polished surfaces. However, G1, G2, and G3 are porous products that are hard to be polished without rubbing off of the particles from their surfaces and embedding of the grinding particles (SiC and/or Al_2O_3) in the surfaces. Furthermore, G1, G2, and G3 have soluble aluminates and silicates on their surfaces that will be contaminated by washing water during the cutting and polishing procedures. Thus, for geopolymers G1, G2, and G3, the SEM/EDX analyses were conducted on their rough fractured surfaces, which inevitably gave errors originating from the false reading of microholes and/or microcrystalline particles on their surfaces.

3.4. TEM and HREM analyses

Figs. 10 and 11 depict the TEM image and diffraction pattern (DP), respectively, of kaolinite powder taken by a Phillips EM 420 TEM. The triclinic hexahedral shapes and hexahedral DP are observed from Figs. 10 and 11, respectively. The obtained DP (Fig. 11(b)) from a kaolinite single crystal matched well with the theoretically simulated DP of kaolinite (Fig. 11(a)).

Figs. 12 and 13 show the stilbite TEM image and DP, respectively. Stilbite has triangular and fourlings shapes. The DP of stilbite (Fig. 13(b)) was observed to match the theoretically simulated DP (Fig. 13(a)) as well. Figs. 10–13 show that TEM images and DP patterns offer an opportunity to view, select, and analyse particles on a microscale.

Figs. 14 and 15 show DP of gel particles. The DP with a dotted ring shape (Fig. 14) is interpreted as a semicrystalline particle and the DP with a cloudy ring (Fig. 15) shape is produced by an amorphous particle.

TEM/EDX analyses for the gel phases of G1 and G3 were carried out as follows:

1. Find a gel particle with irregular shape at 12.7 k magnification.
2. Perform an electronic diffraction on the selected particle to see whether it is amorphous or not.

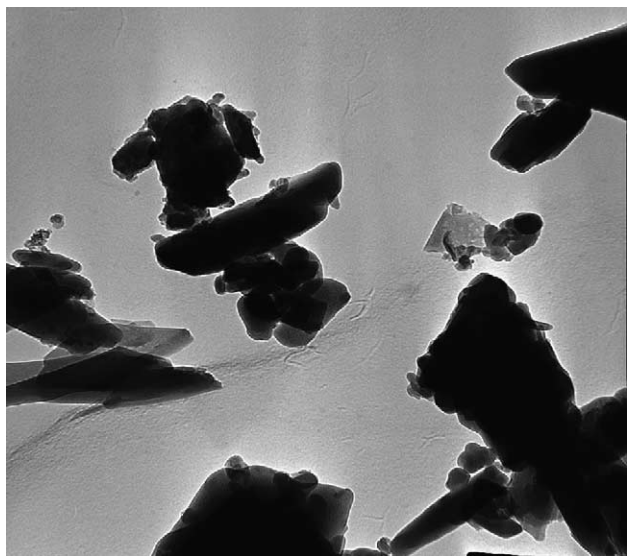

Fig. 12. TEM image of stilbite at a magnification of $\times$ 36,300.

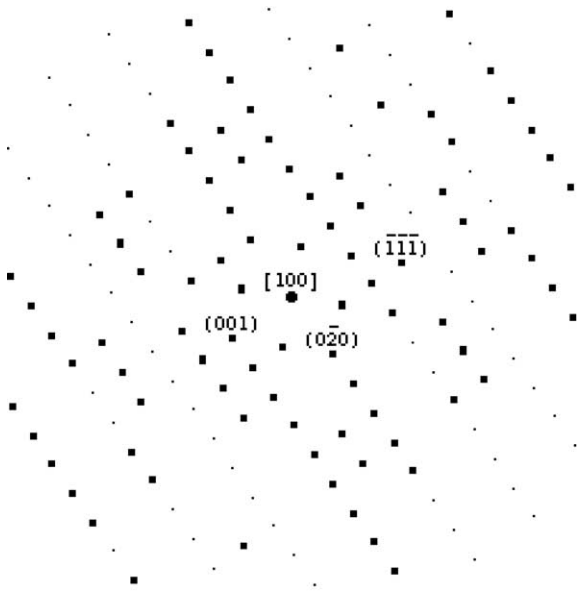

(a) Simulated DP of stilbite

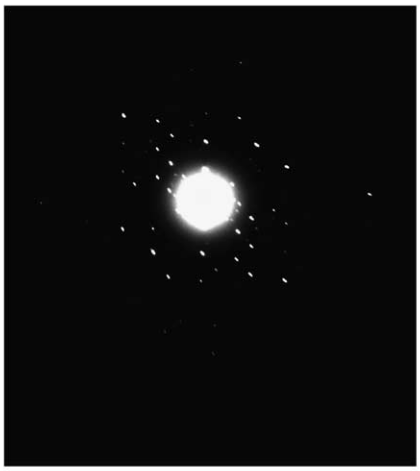

(b) DP of stilbite

Fig. 13. Simulated and real DP of stilbite particle.

3. After identifying the particle as an amorphous gel particle, perform an EDX analysis.
4. Repeat the above procedures (1) to (3) 15 times to determine the variability of results.

Table 5 shows the mean results obtained from TEM/EDX analyses for G1 and G3. During the analysis of TEM/EDX, the Cliff–Lorimer factor [21] K_{SiAl} has been calculated by using the stoichiometry of kaolinite (CMS KGa-1). Thus, only Al_2O_3 and SiO_2 values calculated from the Al and Si counts are reported in Table 5. The values of Al_2O_3 weight percentage and SiO_2 weight percentage for G1 and G3 listed in Table 5 are close to the values shown in Table 4. It is noteworthy that the values of S.D. are lower in Table 5 than in Table 4. Consequently, it is observed that both

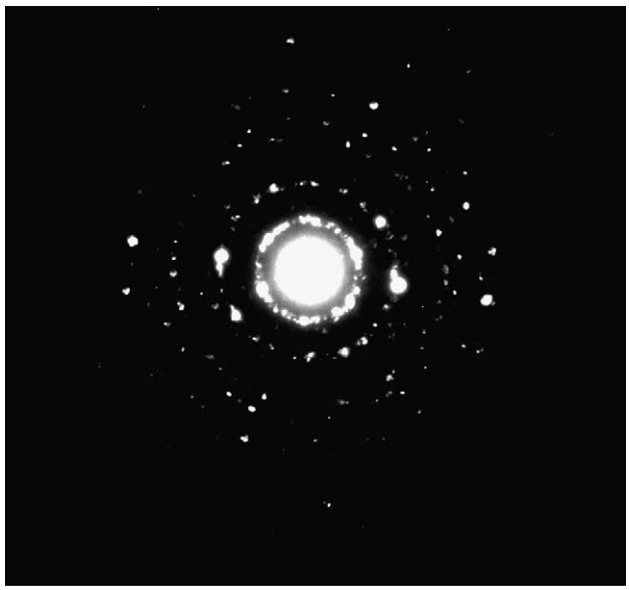

Fig. 14. DP of semicrystalline geopolymer formed by kaolinite/stilbite mixture.

SEM/EDX and TEM/EDX are reliable techniques for semiquantitative analysis of the gel compositions of G1 and G3, but that TEM/EDX has higher reproducibility and can be considered as more accurate. The reason why TEM/EDX is more accurate than SEM/EDX for the analysis of gel is that the TEM/EDX technique can analyse individual particles after identification of the amorphous gel phase, which avoids false reading from any other crystalline phases or microholes.

The investigation results obtained from XRD and ^{27}Al and ^{29}Si MAS-NMR suggest that stilbite particles are completely dissolved during the geopolymerisation of G1

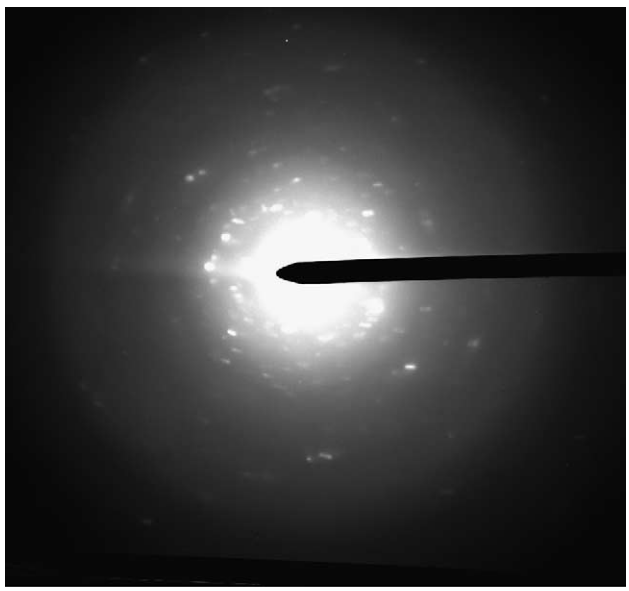

Fig. 15. DP of amorphous geopolymer formed by kaolinite/stilbite mixture.

Table 5
Composition of gel phase in geopolymers (G1 and G3) obtained from TEM/EDX analyses

Element as oxide (wt.%)	G1		G3	
	Mean	S.D.	Mean	S.D.
Al_2O_3	25.96	2.79	19.22	2.71
SiO_2	64.7	3.59	62.75	1.8

and kaolinite particles are totally transferred into the gel of G3. Therefore, a calculation for the structural compositions of G1 and G3 can be conducted based on the assumptions that there are no new crystalline products and precipitates formed during the geopolymerisation of G1 and G3, and that the added sodium silicate stayed in the gel phase. Eq. (1) schematically describes the geopolymerisation from kaolinite/stilbite mixtures:

$$\begin{gathered}\text{Kaolinite (s)} + \text{Stilbite (s)} + \text{Sodium silicate solution} + \text{NaOH solution} \\ \Downarrow \\ \Downarrow \\ \text{Geopolymer} \\ \text{(undissolved solid particles} + \text{gel phase)}\end{gathered} \quad (1)$$

The Al_2O_3 and SiO_2 contained in the gel can be expressed as Eqs. (2) and (3), respectively.

$$SiO_2\ (K) + SiO_2\ (St) + SiO_2\ (So) = SiO_2\ (Gel) \quad (2)$$

$$Al_2O_3\ (K) + Al_2O_3\ (St) = Al_2O_3\ (Gel) \quad (3)$$

where SiO_2 (K) represents SiO_2 dissolved from kaolinite powder, SiO_2 (St) represents SiO_2 dissolved from stilbite particles, SiO_2 (So) represents SiO_2 added from sodium silicate solution, SiO_2 (Gel) represents SiO_2 contained in gel phase, Al_2O_3 (K) represents Al_2O_3 dissolved from kaolinite powder, Al_2O_3 (St) represents Al_2O_3 dissolved from stilbite particles, and Al_2O_3 (Gel) represents Al_2O_3 contained in the gel phase. The weight percentages of Al_2O_3 and SiO_2 in kaolinite, stilbite, and gel phases of G1 and G3 can be obtained from Tables 1 and 5, respectively. The added SiO_2 (So) is calculated as 1.3 ml × 1.385 g/ml × 28.65 wt.%, which gives 0.516 g of SiO_2 (So).

The total start solid mixture weighs 21 g and the kaolinite/stilbite mass ratio for G1 and G3 is 6.5 and 0.1, respectively, so that 2.8 g of stilbite and 1.91 g of kaolinite have been transferred, respectively, into the gel phases of G1 and G3. Thus, Eqs. (2) and (3) can be expressed for the case of G1 as:

$$2.8 \times 59.2\% + X \times 54.5\% + 0.516 = Y \times 64.7\% \quad (4)$$

$$2.8 \times 14.8\% + X \times 29.4\% = Y \times 25.96\% \quad (5)$$

and for the case of G3 as:

$$1.91 \times 54.5\% + Z \times 59.2\% + 0.516 = W \times 62.75\% \quad (6)$$

$$1.91 \times 29.4\% + Z \times 14.8\% = W \times 19.22\% \quad (7)$$

where X represents the grams of kaolinite dissolved into the gel phase of G1, Y represents the total grams of the gel phase of G1, Z represents the grams of stilbite dissolved in the gel phase of G3, and W represents the total grams of the gel phase of G3.

When Eqs. (4) and (5) or Eqs. (6) and (7) are combined, X and Z can be solved as:

$$X = 6.1\ \text{g} \quad (8)$$

$$Z = 2.5\ \text{g} \quad (9)$$

So the dissolved kaolinite and stilbite in the geopolymerisation of G1 and G3 are 6.1 and 2.5 g, respectively. The structural composition of G1 is 12.1 g of kaolinite particles and 8.5 g of gel. In other words, G1 is composed of 58.7 wt.% of crystalline particles and 41.3 wt.% of amorphous gel. G3 consists of 77 wt.% of crystalline stilbite particles and 23 wt.% of amorphous gel phase. It has been noted that G1 contains more gel phase than G3. However, G1 also showed lower compressive strength than G3 (Table 2), which suggests that other factors such as the ratio of (average surface area)/gel, CaO weight percentage in the gel and the interwovenness of crystalline particles with gel may also affect the final mechanical strengths of G1 and G3.

The calculated average surface areas of the particles contained in G1 and G3 by using average particle sizes and densities of kaolinite and stilbite are 6.82×10^4 and

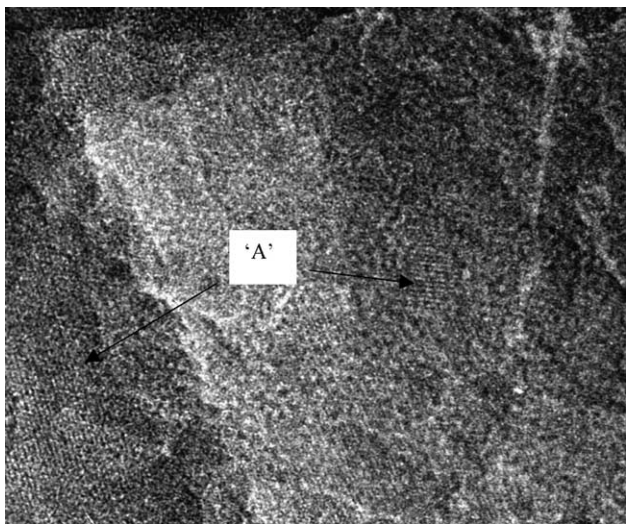

Fig. 16. HREM image of G1 with "A" showing kaolinite crystal particle.

2.35×10^4 cm^2, respectively. It is noticed that the surface area of the particles contained in G1 is 2.9 times the surface area of the particles in G3. Also, the calculated ratio of (average surface area)/gel in G1 is found to be 1.64 times that in G3. Hence, it is found that although G1 contains more gel phase than G3, it has a higher ratio of (average surface area)/gel as well. A higher ratio of (average surface area)/gel means on average a thinner gel layer between the undissolved particles in G1. Therefore, the reasons why G1 shows lower compressive strength than G2 and G3 may be not only the weaker gel phase but also the higher ratio of (average surface area)/gel. Besides the lower CaO weight percentage contained in the gel and the higher ratio of (average surface area)/gel in G1, the lower hardness (2.5 Mohs) of the remaining kaolinite particles may also negatively affect the mechanical strength of G1.

However, it has to be stated that the analyses of SEM/EDX and TEM/EDX conducted here are only at a semiquantitative level, as the analyses cover only a very small part of the corresponding bulk geopolymer. Considering that other practical techniques cannot distinguish the crystalline phases from the amorphous gel, such a semiquantitative method is satisfactory for providing some insight into the structural composition of geopolymers. The interpretation of the results obtained from semiquantitative SEM/EDX and TEM/EDX analyses can also aid in the understanding of the factors affecting the final compressive strength of a geopolymer. The method developed in the present work is also applicable to other related materials such as cement and concrete.

Figs. 16 and 17 are the images of G1 and G3 taken by HREM. It has been observed that both G1 and G3 are composed of amorphous gel and crystalline particles. The crystal lattice of kaolinite can be observed (“A”) in Fig. 16, while only a distorted crystal lattice of stilbite is found in Fig. 17 (“B”). A quick shift from a regular crystal lattice image to a disordered amorphous image is observed throughout the HREM investigations for both kaolinite and stilbite particles. In particular, the crystalline stilbite is found to have a quicker shift than that of kaolinite, which is also the reason why only an image of a distorted crystal lattice was recorded for stilbite. The phenomenon of the shifts of crystal lattice suggests that beam damage happened for both kaolinite and stilbite during the HREM studies. The shifts of crystal lattice observed during HREM analyses also suggest that the energy gaps between crystalline kaolinite or stilbite and their amorphous structures are not large, which may be the reason why these two minerals have high reactivity in geopolymerisation. In spite of beam damage that will transfer part of the crystalline kaolinite and stilbite particles into the amorphous phase, the HREM studies of G1 and G3 have proven at the microcrystal level that only amorphous and kaolinite or stilbite characteristic crystal lattices are observed in G1 and G3, respectively.

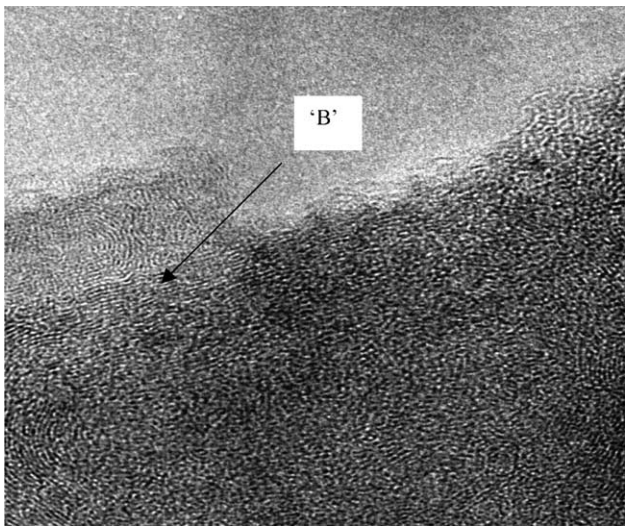

Fig. 17. HREM image of G3 with “B” showing stilbite crystal particle.

4. Conclusion

When an excess of stilbite is present in a mixture of stilbite and kaolinite, a fraction of the stilbite remains as a crystalline phase interspersed in a continuous amorphous geopolymeric phase. When the stilbite is deficient, the kaolinite remains partially dissolved in the gel phase. XRD and ^{29}Si and ^{27}Al MAS-NMR were used to show the characteristic DP and chemical shifts, respectively, for the remaining crystalline phase. TEM electron diffraction and HREM were used to establish the amorphous nature of the formed continuous gel phase. SEM, TEM, and HREM could also be used to identify the undissolved mineral phases. TEM/EDX was shown to give a more reliable microanalysis of the composition of the gel phase than SEM/EDX. The mean composition of the continuous gel phase was used in a simple mass balance equation to calculate the quantity of gel formed and the associated amount of partially reacted mineral, if it was assumed that one mineral in a binary system dissolved completely. For example, a geopolymer synthesised at the kaolinite/stilbite mass ratio of 6.5 was found to contain 58.7 wt.% of crystalline kaolinite particles and 41.3 wt.% of gel phase. At the kaolinite/stilbite mass ratio of 0.1, the produced geopolymer was composed of 77 wt.% of crystalline stilbite particles and 23 wt.% of gel phase. It was also found that the compressive strength of a geopolymer increased as a higher CaO wt.% was present in its gel, a lower ratio of (average surface area)/mass of gel was developed, and where the remaining crystalline particles had a higher hardness. These observations will provide the basis for an improved understanding of geopolymer technology and the characterisation of source materials. The method developed in the present work could also be used in other related materials such as conventional concrete.

Acknowledgements

The authors wish to thank Dr. Simon Ringer, Dr. Steven P. Swenser, and Mr. Renji Pan of Monash University for valuable discussion and assistance in microscopic analysis. The financial support of the Australian Research Council is greatly appreciated.

References

[1] J. Davidovits, Geopolymers: Inorganic polymeric new materials, J. Therm. Anal. 37 (1991) 1633–1656.
[2] J. Davidovits, Geopolymers: Inorganic polymeric new materials, J. Mater. Educ. 16 (1994) 91–139.
[3] A. Palomo, A. Maclas, M.T. Blanco, F. Puertas, Physical, chemical and mechanical characterisation of geopolymers, Proc. 9th Int. Congr. Chem. Cem. (1992) 505–511.
[4] A. Palomo, M.T. Blanco-Varela, M.L. Granizo, F. Puertas, T. Vazquez, M.W. Grutzeck, Chemical stability of cementitious materials based on metakaolin, Cem. Concr. Res. 29 (1999) 997–1004.
[5] J.G.S. Van Jaarsveld, J.S.J. Van Deventer, L. Lorenzen, The potential use of geopolymeric materials to immobilise toxic metals: Part I. Theory and applications, Miner. Eng. 10 (1997) 659–669.
[6] J.G.S. Van Jaarsveld, J.S.J. Van Deventer, A. Schwartzman, The potential use of geopolymeric materials to immobilise toxic metals: Part II. Material and leaching characteristics, Miner. Eng. 12 (1998) 75–91.
[7] H. Xu, J.S.J. Van Deventer, The geopolymerisation of alumino-silicate minerals, Int. J. Miner. Process. 59 (2000) 247–266.
[8] A. Palomo, M.W. Grutzeck, M.T. Blanco, Alkali-activated fly ashes, a cement for the future, Cem. Concr. Res. 29 (1999) 1323–1329.
[9] A. Fernández-Jiménez, J.G. Palomo, F. Puertas, Alkali-activated slag mortars, mechanical strength behaviour, Cem. Concr. Res. 29 (1999) 1313–1321.
[10] J.W. Phair, J.S.J. Van Deventer, J.D. Smith, Mechanism of polysialation in the incorporation of zirconia into fly ash-based geopolymers, Ind. Eng. Chem. Res. 39 (2000) 2925–2934.
[11] X.F. Gao, Y. Lo, C.M. Tam, C.Y. Chung, Analysis of the infrared spectrum and microstructure of hardened cement paste, Cem. Concr. Res. 29 (1999) 805–812.
[12] G. Davies, R.E. Oberholster, Alkali–silica reaction products and their development, Cem. Concr. Res. 18 (1988) 621–635.
[13] A. Iob, H. Saricimen, S. Narasimhan, N.M. Abbas, Spectroscopic and microscopic studies of a commercial concrete water proofing material, Cem. Concr. Res. 23 (1993) 1085–1094.
[14] J.B. Nagy, P. Bodart, H. Collette, C. Fernandez, Z. Gabelica, Characterisation of crystalline and amorphous phases during the synthesis of (TPA, M)-ZSM-5 zeolites (M = Li, Na, K), J. Chem. Soc. Faraday Trans. I 85 (9) (1989) 2749–2769.
[15] N. Shigemoto, S. Sugiyama, H. Hayashi, K. Miyaura, Characterisation of Na–X, Na–A, and coal fly ash zeolites and their amorphous precursors by IR, MAS NMR and XPS, J. Mater. Sci. 30 (1995) 5777–5783.
[16] M. Enders, Microanalytical characterisation (AEM) of glassy spheres and anhydrite from a high-calcium lignite fly ash from Germany, Cem. Concr. Res. 25 (1995) 1369–1377.
[17] S. Gomes, M. François, M. Abdelmoula, Ph. Refait, C. Pellissier, O. Evrard, Characterisation of magnetite in silico-aluminous fly ash by SEM, TEM, XRD, magnetic susceptibility, and Mössbauer spectroscopy, Cem. Concr. Res. 29 (1999) 1705–1711.
[18] S. Gomes, M. François, Characterisation of mullite in silicoaluminous fly ash by XRD, TEM, and ^{29}Si MAS NMR, Cem. Concr. Res. 30 (2000) 175–181.
[19] B. Velde, Electron microprobe analysis of clay minerals, Clay Miner. 19 (1984) 243–247.
[20] E.H. Nickel, M.C. Nichols, Mineral Reference Manual, Van Nostrand Reinhold, New York, 1991.
[21] G. Cliff, G.W. Lorimer, The quantitative analysis of thin specimens, J. Microsc. 103 (1975) 203–207.